Preliminary shielding results for the ESRF storage ring upgrade

P. Berkvens, L. Farvacque, R. Versteegen

ESRF, 38043 Grenoble Cedex 9, France

Abstract

The ESRF Council has approved the ESRF Phase II Upgrade Programme that will be implemented in the 2015 – 2022 period. Within this programme, a major upgrade of the storage ring is planned, to reduce the storage ring's equilibrium horizontal emittance and consequently increasing the brilliance of the X-ray beams.
The paper deals with the preliminary shielding study for the new storage ring. Due to the decreased beam emittance, the expected beam lifetimes will be significantly reduced compared to the present storage ring. As a consequence, the existing bulk storage ring tunnel shielding will not be sufficient to allow maintaining the ESRF radiation protection policy – 2 μSv per 4 hours. Special beam loss collimators will therefore be inserted in the lattice. The presentation describes the optimisation of these collimators.

1. Introduction

The present storage ring tunnel shielding allows the operation of the storage ring under most practical conditions within the ESRF radiation protection policy (all people working at the ESRF to be considered as non-exposed workers, with a derived dose constraint of 2 μSv/4h). It should be recalled that thanks to this radiation protection policy, ESRF does not need to organize a personal dosimetry follow up.
Detailed shielding measurements carried out at the end of the 1990s have allowed us to characterize the shielding capacity of the storage ring. The following shielding factors were obtained:

- Photons: 0.8 $\mu Sv \cdot kJ^{-1}$
- Neutrons: 1.6 $\mu Sv \cdot kJ^{-1}$

These relatively low values (these values are more than 1 order of magnitude smaller than theoretical values obtained from a simple analytical point loss model) can be explained on the one hand due to an important self-shielding effect from the important dipole yokes, but, more importantly, due to the fact that actual beam losses are always distributed over a more or less large distance, typically 10 – 15 meters, from the ID vessel into the achromat.
The large beam lifetime and the large mean time between failures, together with these favorable shielding factors, explain why the 4-hour dose interlock of the injector has never been tripped during normal operation. During accelerator R&D operation, because of the much higher injected charge during some shifts, the dose interlock trips from time to time.
The situation has to be reassessed with the new lattice. The expected much smaller lifetime and possibly the fact that the actual beam losses may occur over shorter distances could result in a situation where the 4-hour dose value could be easily exceeded during normal user operation.

2. Comparative Shielding Study

Since one of the boundary conditions of the phase II upgrade is to use as much as possible existing infrastructures, the shielding study for the new storage ring must demonstrate that it will indeed be possible to operate the new facility without major upgrades of the existing shielding. One of the basic radiation protection requirements is the ALARA principle (As Low As Reasonably Achievable). The shielding study must therefore clearly demonstrate how ESRF applies the ALARA principle to minimize radiation hazards for workers, for the public and for the environment. In this context, the operation of the new facility without major reinforcement of the existing shielding can only be justified if one can show that the present ESRF radiation protection policy, which guarantees the non-exposure of all people working at the ESRF, can be maintained.
Preliminary shielding calculations have been carried out, comparing the existing lattice with the new lattice. FLUKA [1] simulations were therefore made for the existing lattice and for the new lattice. In the standard cells of the existing lattice primary electron losses are essentially concentrated on the input taper of the insertion device vessels. For the new lattice, in the absence of specific collimators those input tapers will also

act as the smallest vertical limiting apertures. Electron losses for the comparative study were therefore assumed to take place on these tapers. Figure 1 shows the total (photon + neutron) dose distribution in a horizontal plane at beam height for both lattices, corresponding to one primary electron lost. One can see that the dose distributions outside the shield walls are very similar in both cases. This is further illustrated in figure 2, showing the residual dose values behind the ratchet wall, the inner wall and above the roof.

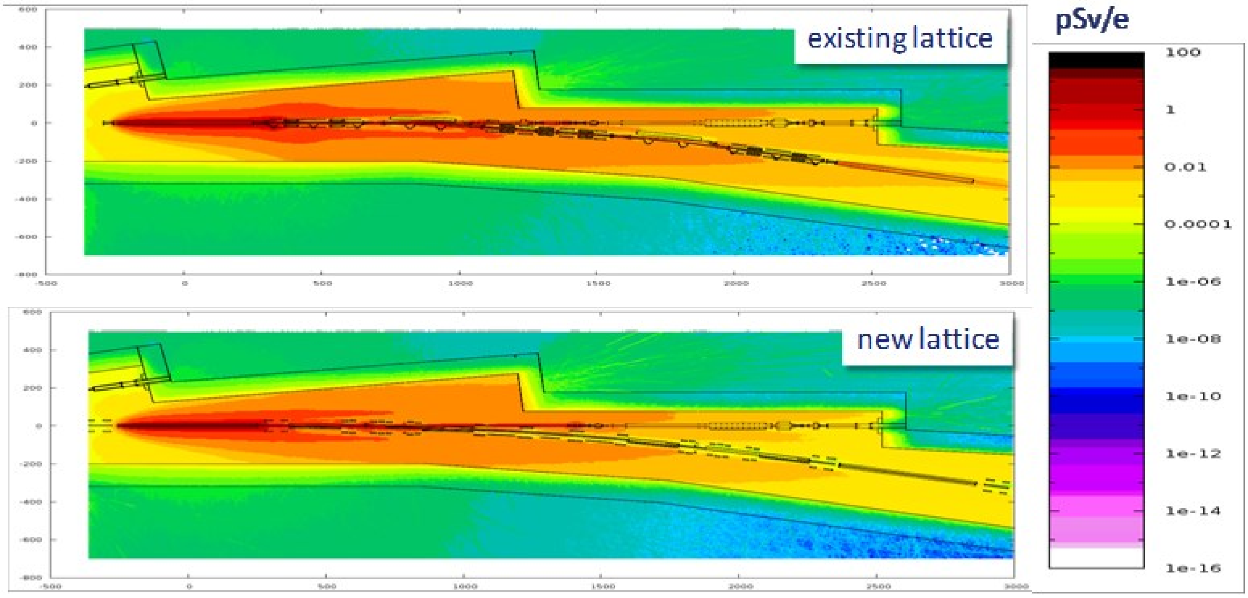

Fig.1 – Comparison between the dose distributions for the existing and new storage ring (residual dose rates per electron lost).

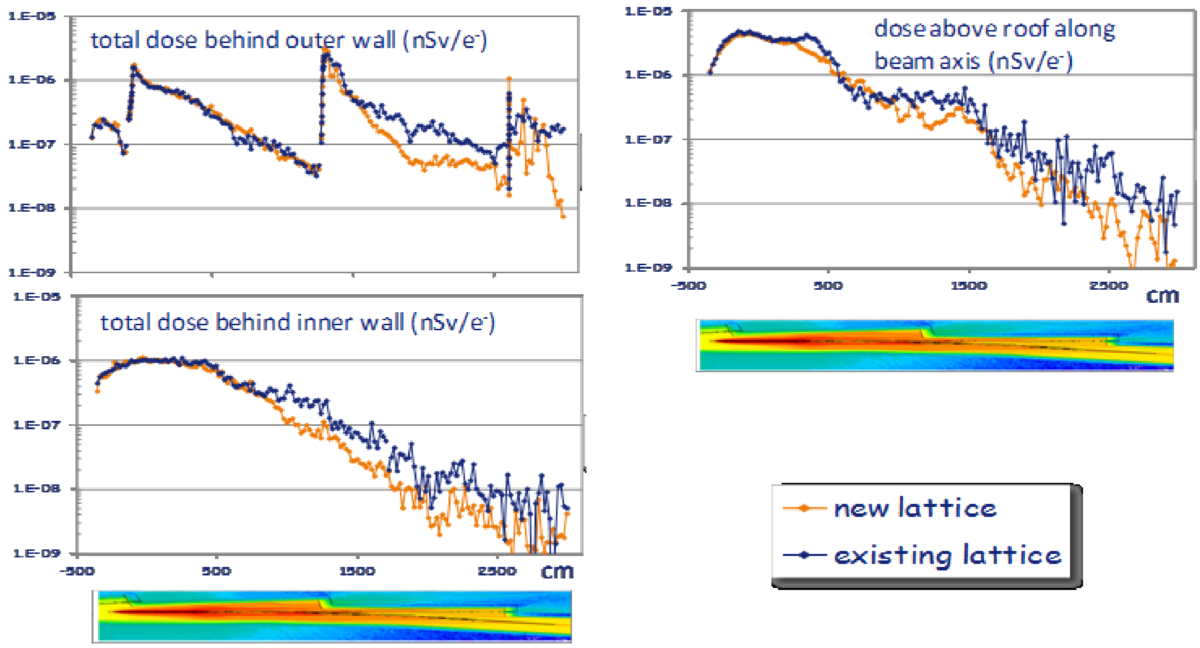

Fig.2 – Comparison between the dose values outside the tunnel for the existing and new storage ring (residual dose rates per electron lost).

We next compare the expected dose rates during normal operation of the two lattices. The highest dose rates are expected in 16-bunch mode. With the present lattice a lifetime of 16 h at 90 mA is obtained. Beam loss measurements show that local beam losses in standard cells, i.e. cells other than the injection cell and cell 5 where the scrapers are installed, are typically of the order of 1 %, reaching values of the order of 10 % for cells having in-vacuum undulators when the latter are operated at minimum gap. For the new lattice, the calculated lifetime at 90 mA is 2.4 h. The corresponding dose rate distributions behind the walls and above the roof are shown in figure 3.

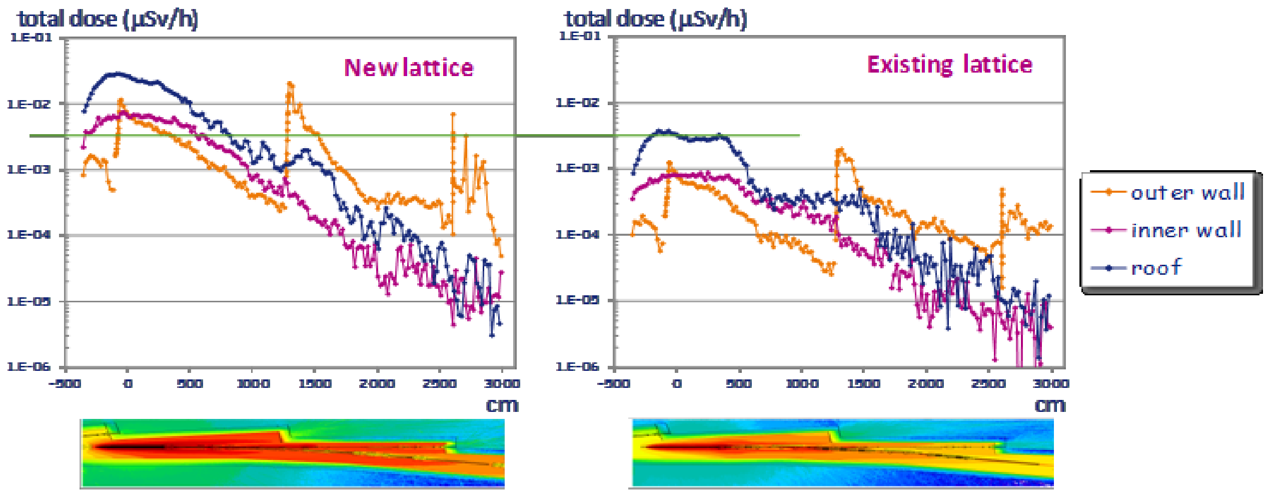

Fig.3 – Comparison between the dose rates outside the storage ring tunnel for the existing and new storage ring. New lattice: 90 mA – 2.4 h lifetime, topping up, 1% local losses – Existing lattice: 90 mA – 16 h lifetime, average over 4 hours decay, 1% local losses

3. Beam loss collimators

The results in figure 3 show that for the new lattice, especially above the roof, dose rates will be too high if local losses of the order of 10 % will occur, especially when assuming non optimal injection efficiencies. We therefore decided to try to localize the losses in a few places around the ring, by installing dedicated beam loss collimators. Beam dynamics studies have indeed shown that the insertion of 2 beam loss collimators along the ring allow to concentrate about 80 % of the total losses on these scrapers [2].
To optimize the collimators from a radiation protection point of view, we used as a figure of merit the reduction of the photon and neutron radiation escaping from the collimator. Figure 4 shows the photon and neutron energy flux escaping the rear face of a tungsten and a copper target, as a function of the target thickness. The results show the superior behavior of tungsten compared to copper and also show that one needs a few 10s of cm of thickness to obtain sufficient attenuation. Due to space constraints, the maximum length we can envisage for the collimators is about 30 cm.

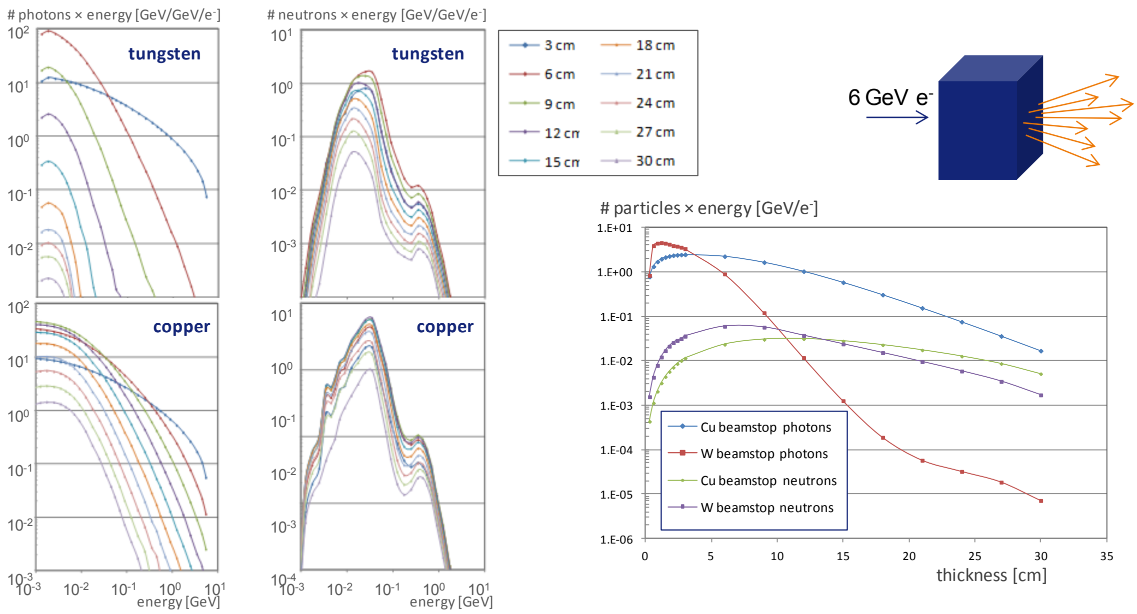

Fig.4 – Photon and neutron radiation escaping from a tungsten and from a copper target bombarded with 6 GeV electrons.

FLUKA simulations were performed to evaluate the performance of different collimator geometries. For these calculations, the phase space distributions of the electrons hitting the slits, as obtained from the beam dynamics studies have been used (see figure 5). The majority of the electrons will hit the slits very close to the edges. Furthermore, due to the optical functions, these electrons are moving towards the edge of the blade, explaining why a non negligible fraction will escape from the blades after a very short distance.

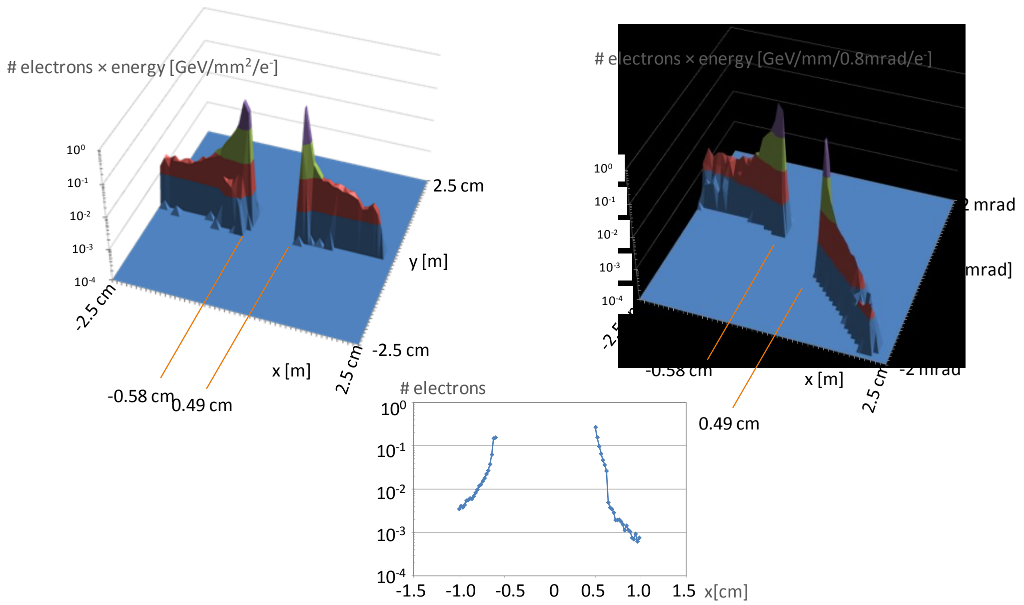

Fig.5 – Phase space distribution (energy fluence) of the electrons intercepted by the collimator.

Theoretically, a very thin collimator (scraper) could also be used. As seen in figure 4, locally very little photons and neutrons are produced in the case of a thin scraper, while the energy of the Touschek scattered electrons hitting the outer blade could be sufficiently reduced to bring them back in the energy acceptance of the storage ring, thereby reducing the electron losses. Unfortunately, from a radiation protection point of view, this solution doesn't work as can be seen in figure 6, showing the dose rate distributions around 1.4 mm thick copper slits (corresponding to an average energy loss of 1 % for 6 GeV electrons). The thin slits indeed result in effective electron losses which are smeared out over several meters downstream of the slits and which are therefore practically impossible to shield.

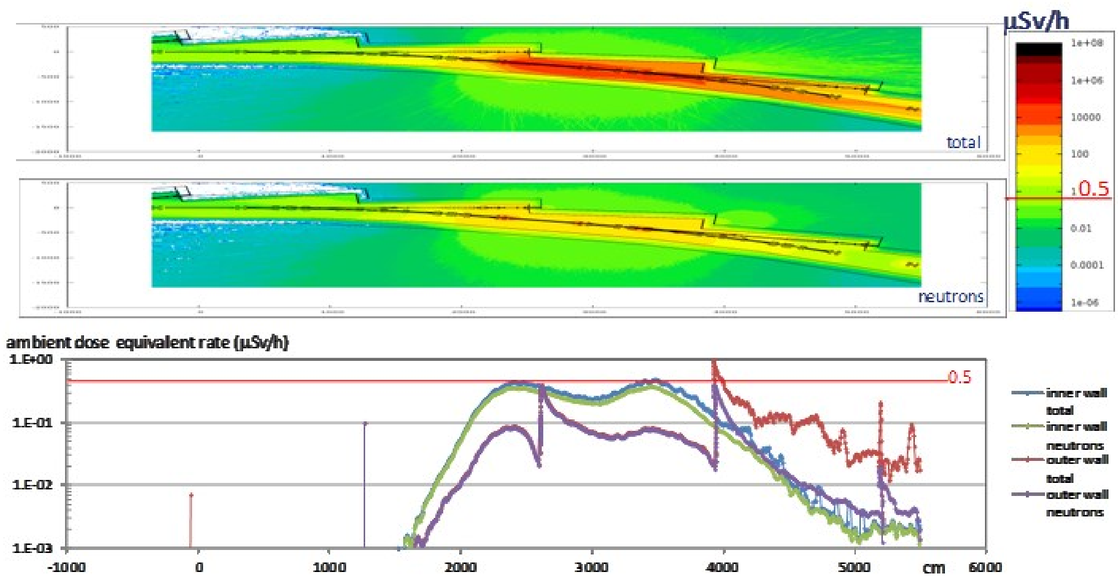

Fig.6 – Dose rate distributions around a 1.4 mm thick copper scraper. Beam parameters: 90 mA – 2.4 h lifetime, topping up, 45 % local losses.

We therefore go for a thick tungsten collimator. Figure 7 compares the energy flux for an optimized collimator, compared to the theoretical case of a beam stop and the simple case of non-tapered slits. The optimization consists in using tapered blades, thanks to the decreasing horizontal β-function inside the collimator, and closing top and bottom of the slits to create a full collimator.

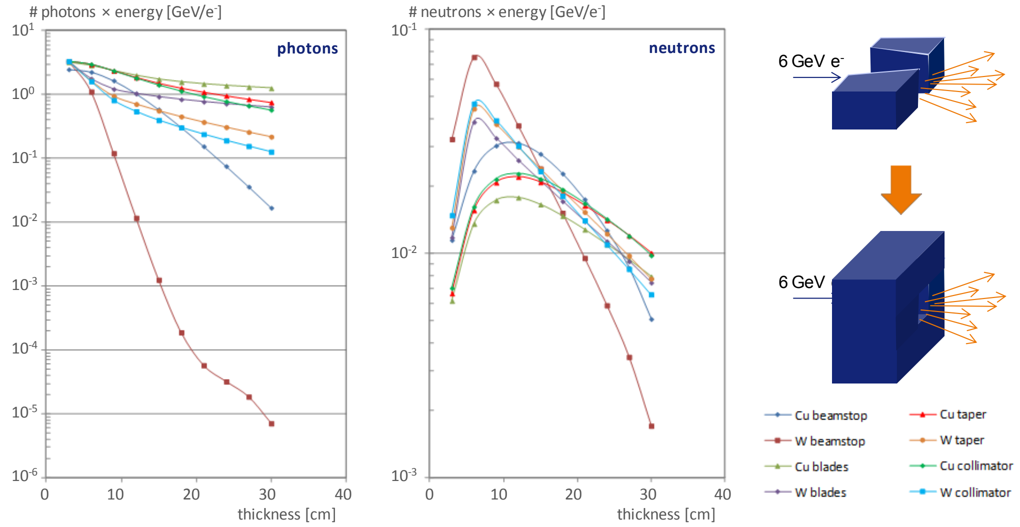

Fig.7 – Comparison between the photon and neutron radiation escaping for different geometries.

To further illustrate the optimization of the collimator, figure 8 shows the photon energy fluence escaping from the collimator. Without changing the angular direction of the escaping photons, we can back trace them to the entrance face of the collimator. The results obtained show that the escaping photons correspond almost exclusively to photons which are created at small depth and at very small distances from the horizontal edges and almost immediately escape. These photons, independent of the geometry of the collimator, will always escape.

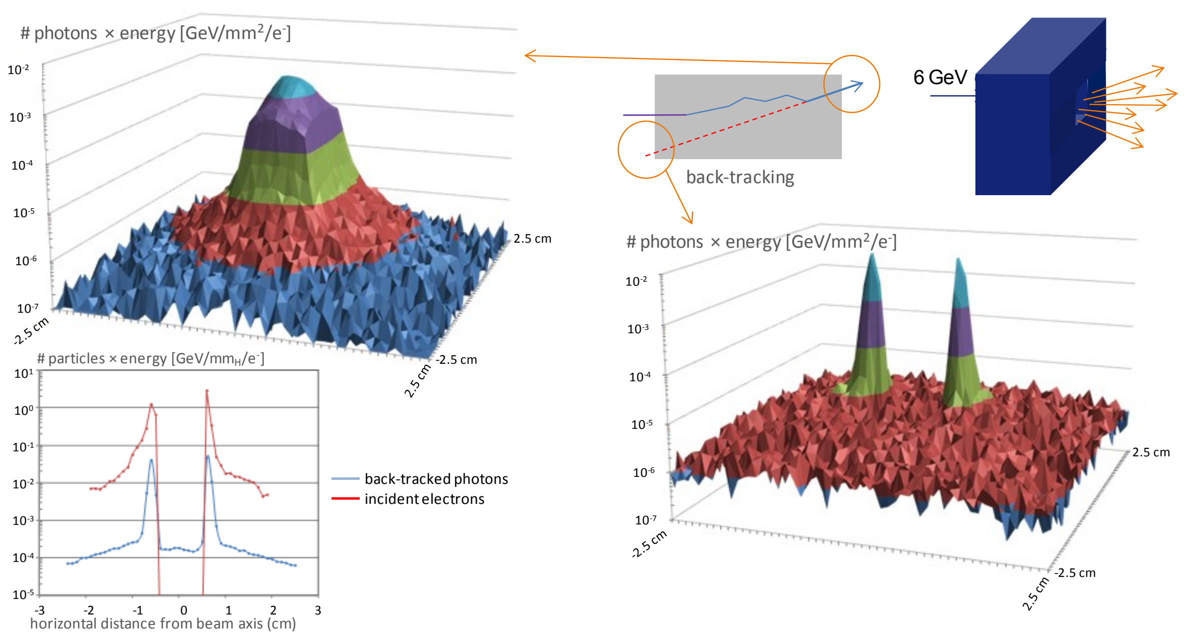

Fig.8 – Optimized collimator: top, left: photon energy fluence at the exit of the collimator. Right, bottom: back traced photon energy fluence, back traced to entrance face of collimator, assuming no scattering inside collimator. Left, bottom: incident and back traced horizontal photon energy fluences.

Figure 9 shows the dose distribution around the 30 cm thick tungsten optimized collimator, without any local shielding. As expected, the dose rates outside the tunnel are too high. However, compared to the results of figure 6, for the thin slits, we see that the dose distribution corresponds this time to a local loss point, clearly illustrating the efficiency of the collimator.

In this case, it will indeed be possible to locally shield the collimator, as shown in figure 10. The results correspond to the case with a local 50 cm thick lead shield. We see that this time we have reduced the dose rates outside the tunnel to values below natural background.

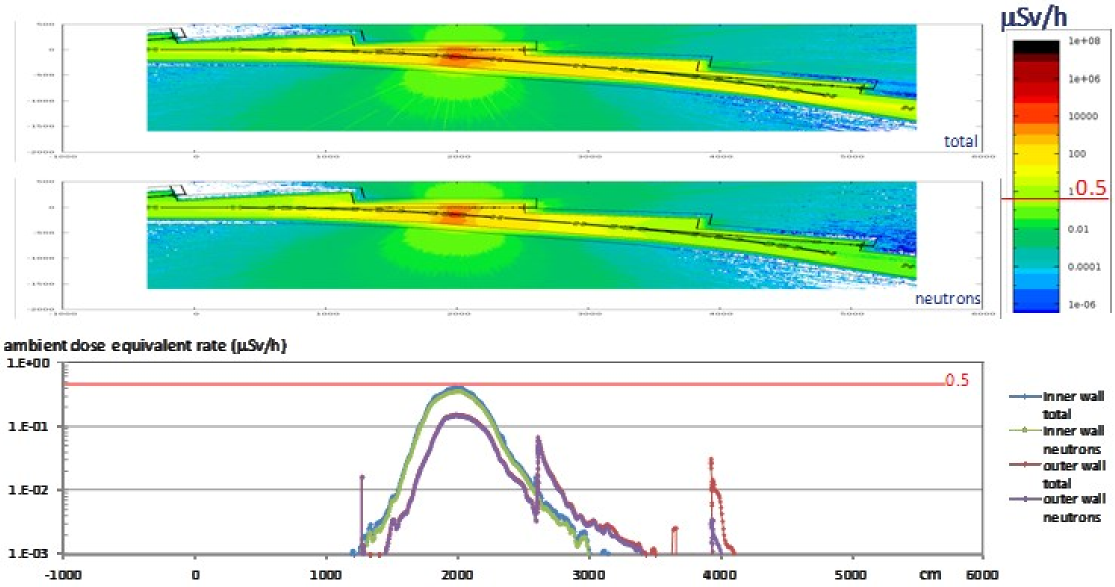

Fig.9 – Dose rate distributions around a 30 cm thick tungsten optimized collimator. Beam parameters: 90 mA – 2.4 h lifetime, topping up, 45 % local losses.

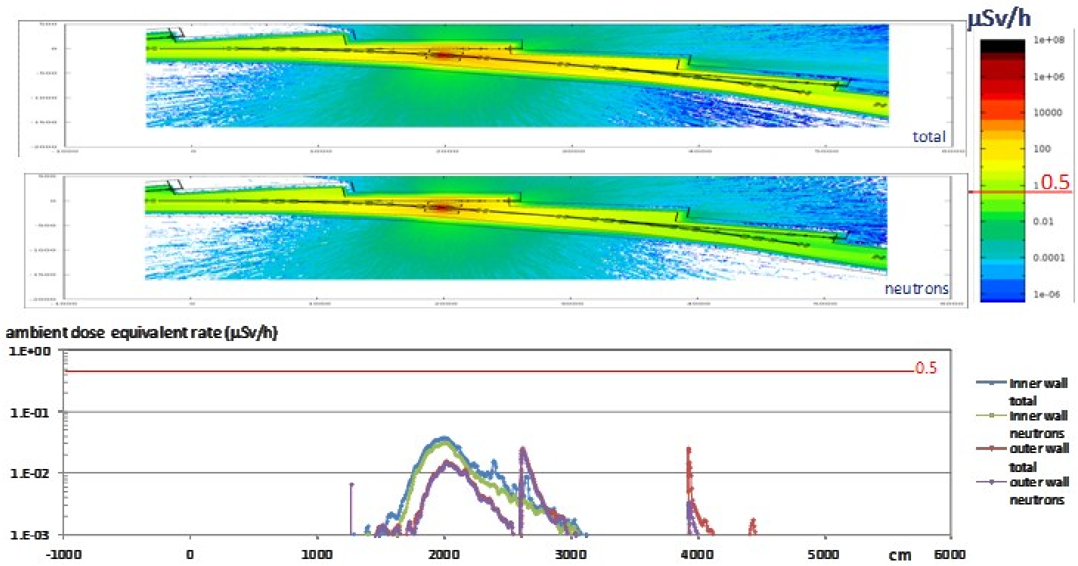

Fig.10 – Dose rate distributions around a 30 cm thick tungsten optimized collimator with 50 cm lead local shielding. Beam parameters: 90 mA – 2.4 h lifetime, topping up, 45 % local losses.

4. Conclusions

The preliminary shielding calculations show that the installation of locally shielded, thick, tungsten beam loss collimators, will allow the operation of the new storage ring while maintaining the present ESRF radiation protection policy (dose rates < 2 µSv per 4 hours). The presence of these collimators will keep the local beam losses in the other cells < 1 %, and no local shielding will be necessary in these standard cells.

References

[1] A. Fassò et al., FLUKA: a Multi-Particle Transport Code, CERN-2005-10,INFN/TC_05/11, SLAC-R-773,2005

[2] R. Versteegen, P. Berkvens, R. Carmignani, L. Farvacque, S.M. Liuzzo, B. Nash, T. Perron, P. Raimondi, S. White, Collimation scheme for the ESRF upgrade, IPAC2015, Jefferson Lab, 3-8 May 2015